Wang, Q., Young, P. & Walters, K. J. Structure of S5a bound to monoubiquitin provides a model for polyubiquitin recognition. J. Mol. Biol. 348, 727–739

ARTICLE *in* JOURNAL OF MOLECULAR BIOLOGY · JUNE 2005

Impact Factor: 4.33 · DOI: 10.1016/j.jmb.2005.03.007 · Source: PubMed

doi:10.1016/j.jmb.2005.03.007 J. Mol. Biol. (xxxx) xx, 1–13

JMB

Available online at www.sciencedirect.com

SCIENCE DIRECT®

ELSEVIER

Structure of S5a Bound to Monoubiquitin Provides a Model for Polyubiquitin Recognition

Qinghua Wang[1], Patrick Young[2] and Kylie J. Walters[1]*

[1]*Department of Biochemistry Molecular Biology and Biophysics, University of Minnesota, 6-155 Jackson Hall 321 Church St SE, Minneapolis MN 55455, USA*

[2]*Molecular Biology and Functional Genomics Stockholm University Stockholm 10691, Sweden*

**Corresponding author*

Ubiquitin is a key regulatory molecule in diverse cellular events. How cells determine the outcome of ubiquitylation remains unclear; however, a likely determinant is the specificity of ubiquitin receptor proteins for polyubiquitin chains of certain length and linkage. Proteasome subunit S5a contains two ubiquitin-interacting motifs (UIMs) through which it recruits ubiquitylated substrates to the proteasome for their degradation. Here, we report the structure of S5a (196-306) alone and complexed with two monoubiquitin molecules. This construct contains the two UIMs of S5a and we reveal their different ubiquitin-binding mechanisms and provide a rationale for their unique specificities for different ubiquitin-like domains. Furthermore, we provide direct evidence that S5a (196-306) binds either K63-linked or K48- linked polyubiquitin, and in both cases prefers longer chains. On the basis of these results we present a model for how S5a and other ubiquitin-binding proteins recognize polyubiquitin.

Keywords: NMR; polyubiquitin; proteasome; S5a; UIM

Introduction

Ubiquitin is a 76 amino acid residue protein that plays a key regulatory role in several prominent biological processes. Well renowned for its role in targeted protein degradation,[1] it can also signal endocytic sorting,[2,3] transcriptional activation and repression,[4,5] DNA repair,[6,7] cell-cycle regulation[8] and other important biological events.[9] The regulatory role of ubiquitin in these and other events begins with its covalent attachment to protein substrates *via* an enzymatic cascade that includes an E1 ubiquitin-activating enzyme, E2 ubiquitin-conjugating enzyme and E3 ubiquitin ligase. As such, ubiquitylation results in an isopeptide bond between a lysine residue of the protein substrate and the C-terminal G76 of ubiquitin. Additional cycles result in a polyubiquitin chain that links G76 to specific lysine residues of the attached ubiquitin moieties.

Unraveling how ubiquitylation can signal distinct events is an active area of research. Two determinants include polyubiquitin chain length and their lysine linkage.[10] Evidence exists for more complicated processing mechanisms. For example, K63-linked chains play a central role in DNA repair[7,11] but can signal proteasome-mediated protein degradation.[12] Furthermore although K48-linked chains trigger targeted protein degradation, distinct receptor pathways are required to funnel ubiquitylated substrates to the proteasome.[13,14] Two such ubiquitin receptors that form alternative pathways to the proteasome in yeast include Rpn10 and Rad23.[13,14]

Proteasome subunit S5a (the human homologue of Rpn10) was the first protein shown to bind polyubiquitin chains;[15] yet, although proteasome proteolysis is essential, Rpn10 is not in budding yeast.[16] This finding has been shown recently to be due to its functional redundancy with DNA repair protein Rad23.[13,14] In fact, the effect of Rpn10 on degradation activities is finely tuned by its relative abundance and requires its ubiquitin-interacting motif (UIM).[13,14]

In humans, S5a and hHR23a/b (the two human homologues of Rad23) may function in a more complicated and collaborative manner to recruit ubiquitylated substrates to the proteasome.[17] A significant fraction of the S5a within a cell is free of the proteasome, and free S5a binds polyubiquitin strongly.[18] It is therefore likely that S5a plays a role similar to that of its yeast homologue in

Abbreviations used: UIM, ubiquitin-interacting motif; UBL, ubiquitin-like; NOE, nuclear Overhauser effect; NOESY, NOE spectroscopy; r.m.s.d., root-mean-square deviation; HSQC, heteronuclear single quantum coherence; UBA, ubiquitin-associated.

E-mail address of the corresponding author: walte048@umn.edu

shuttling ubiquitylated products to the proteasome for their degradation. In contrast to Rpn10, however, S5a contains two UIMs, the second of which (UIM-2) binds hHR23 proteins (Figure 1).[19] This interaction may be regulated by structural changes in hHR23 proteins,[20] which are able to bind S5a and ubiquitin simultaneously.[21] Recently, the structure of a 45 residue S5a peptide containing UIM-2 was solved in complex with the ubiquitin-like (UBL) domain of hHR23a and hHR23b.[22,23] This research provided valuable insight into how UIM-2 of S5a contacts the UBL domain of hHR23a/b. Still

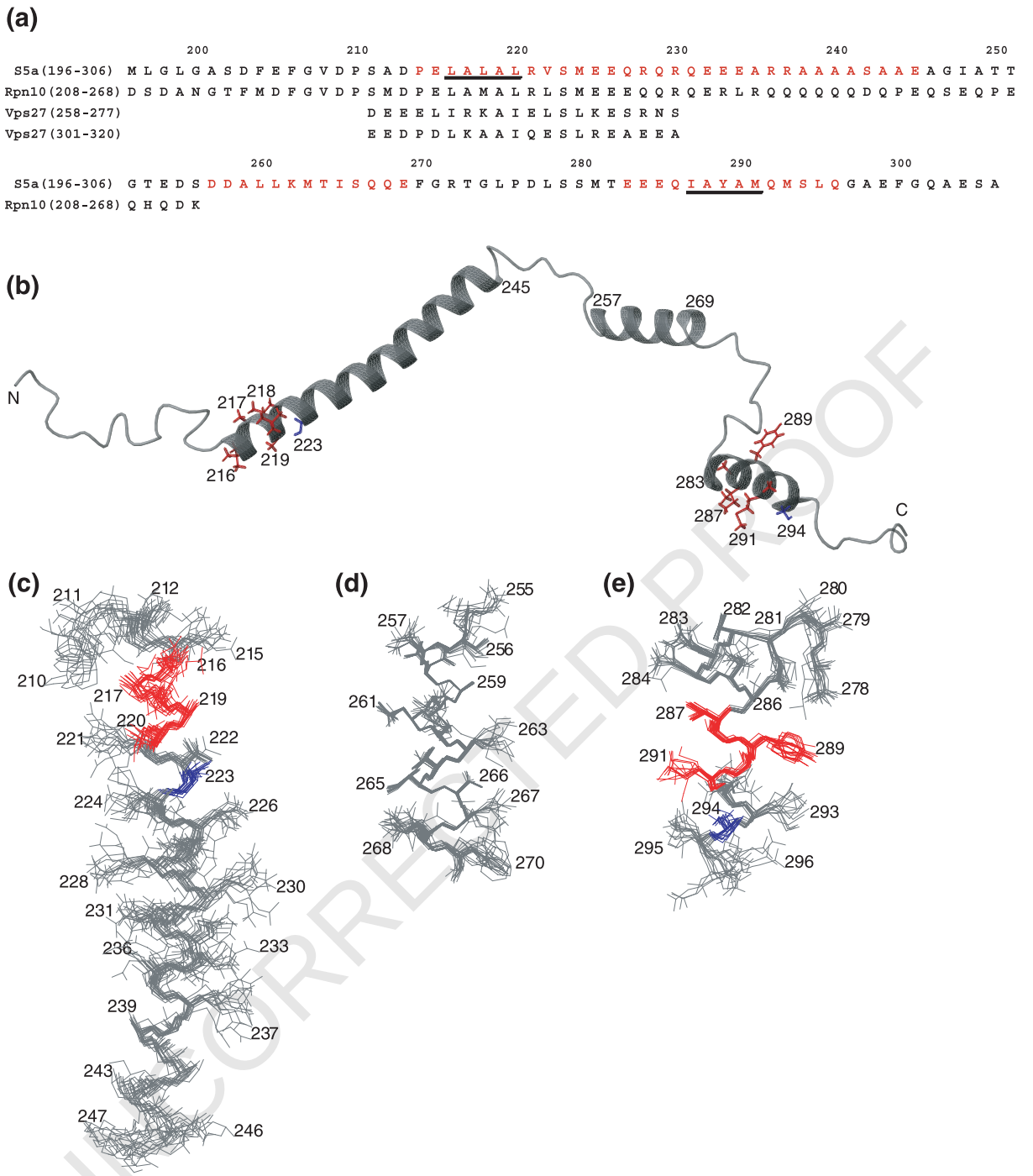

Figure 1. S5a (196-306) contains three α-helices that are connected by flexible regions. (a) The sequence of S5a (196-306), Rpn10 (yeast homolog of S5a) and Vps27 are aligned according to their UIM sequences. The helices of S5a are highlighted with red. A representative structure of S5a (196-306) is provided in (b) and its three well-defined regions are shown in (c), (d) and (e). The average backbone r.m.s.d. from the mean structure for residues P214-E245, D257-E269, and E283-Q296 are 0.786, 0.142 and 0.348 Å, respectively. (b)–(e) The hydrophobic LALAL/IAYAM residues within each UIM are highlighted in red, and the conserved serine residue is colored blue. Parts (b)–(e) were generated by using MOLMOL.[49]

missing, however, is structural information on UIM-1 of S5a and mechanistic knowledge of how either UIM binds ubiquitin and polyubiquitin.

Interestingly the UIMs of S5a have distinct specificity for UBL domain proteins. In particular, whereas S5a binds the UBL domain of hHR23 through UIM-2,[19] it binds that of hPLIC through UIM-1.[24] Furthermore, the UIMs of S5a differ by at least tenfold in their apparent affinity for polyubiquitin chains.[25] How UIMs achieve their distinct specificities for ubiquitin and UBL domain proteins remains to be discovered.

Here, we report the structure of an S5a construct that encompasses both of its UIMs: S5a (196-306). We found significant differences between these two motifs, and we present highly refined structures of their protein complexes with monoubiquitin. In addition, on the basis of our structural data, we hypothesized that S5a (196-306) binds either K63-linked or K48-linked polyubiquitin, and we confirmed these predictions experimentally. Altogether, these results enabled us to propose a model for polyubiquitin recognition and to hypothesize why certain ubiquitin-binding proteins prefer longer polyubiquitin chains.

Results

S5a (196-306) contains three well-defined α-helices that do not interact

To understand how the UIMs of S5a recognize ubiquitin, we solved the structure of S5a (196-306) alone and complexed with ubiquitin. This construct contains both UIMs of S5a (Figure 1(a)), each of which binds polyubiquitin.[25] We expect it to be structurally intact, as the amide nitrogen and proton resonance signals derived from S5a (196-306) appear to be unperturbed relative to those of full-length S5a (see Figure S1 in Supplementary Data).

S5a (196-306) contains three well-structured regions spanning residues P214-E245, D257-E269, and L278-Q296 (Figure 1(b)–(e)). Flexible, randomly coiled linker regions connect the structured elements and prevent them from being defined relative to each other. This lack of higher-order structure within these regions is supported by their chemical-shift assignments,[26] lack of long-range nuclear Overhauser effect (NOE) interactions, and NMR relaxation data (data not shown). As discussed below, the flexibility of the linkers likely facilitates S5a binding to polyubiquitin.

The first helix of S5a (196-306) spans residues P214 to E245 and is comprised of nine helical turns, with the N terminus capped by D213 and P214 (Figure 1). The hydrophobic repeat $L^{216}ALAL^{220}$ for which this UIM is well known resides within the first two helical turns (Figure 1(c)). Interestingly, a significant number of charged residues alternate in the helix, including R221, E225, E226, R228, R230, E232, E233, E234, R236, and R237. This stretch may have functions similar to those of KEKE motifs, which are suggested to promote interactions between proteins.[27]

The third structural element contains UIM-2, which is characterized by the hydrophobic repeat $I^{287}AYAM^{291}$, and includes an α-helix spanning residues E283 to Q296. N-terminal to this helix is a turn comprising L278-T282. This region is defined by 28 long-range interactions between P276, L278, M281, Q286, and Y289. These residues form a hydrophobic surface, whereas neighboring D277, S279, S280, and T282 comprise the opposite hydrophilic surface. Each of the three α-helices in S5a (196-306) begins with negatively charged residues, which are known to promote helix formation.[28] One striking difference between UIM-1 and UIM-2 is the positioning of the hydrophobic LALAL/IAYAM sequence. In UIM-1 this sequence is positioned at the N-terminal end of the α-helix, whereas in UIM-2 it resides in the second and third helical turn, as highlighted in Figure 1. As discussed below, this structural difference likely contributes to UIM-2 serving as the preferred mono- and polyubiquitin-binding partner.

UIM-2 of Vps27 formed a tetramer when it crystallized, although it was monomeric in solution.[29] This contradiction led us to test our hypothesis that the UIMs of S5a do not interact with each other, as indicated by the lack of NOE interactions between the three structured elements of S5a (196-306). We expressed separately protein constructs containing either UIM-1 (S5a (107-241)) or UIM-2 (S5a (263-307)). We then mixed these constructs and tested for their interaction by using NMR chemical shift perturbation studies and gel-filtration studies (data not shown). Each of these techniques confirmed that these two regions do not interact. To test for UIM-1/UIM-1 and UIM-2/UIM-2 interactions, we extended these studies by expressing a longer S5a protein construct: S5a (107-306). Similarly, gel-filtration experiments revealed this construct did not interact with S5a (196-306) (data not shown). Furthermore, sedimentation velocity analysis on S5a (196-306) at concentrations ranging from 0.2 mg/ml to 2 mg/ml indicated that it is monomeric. Altogether, these data offer strong support for S5a (196-306) being monomeric in solution, and for its two UIMs not interacting with each other, which is consistent with published data indicating that the two UIMs of Vps27 are autonomous in solution.[30]

A simple approach to define the contact surfaces between S5a (196-306) and ubiquitin

We implemented a simple method for assigning intermolecular NOE interactions to be used in conjunction with previously published techniques. In particular, we produced $^{15}N,^{2}H$-labeled S5a (196-306) and mixed it with either unlabeled or ^{13}C-labeled ubiquitin. With the sample containing unlabeled ubiquitin we acquired a standard ^{15}N-dispersed NOE spectroscopy (NOESY)

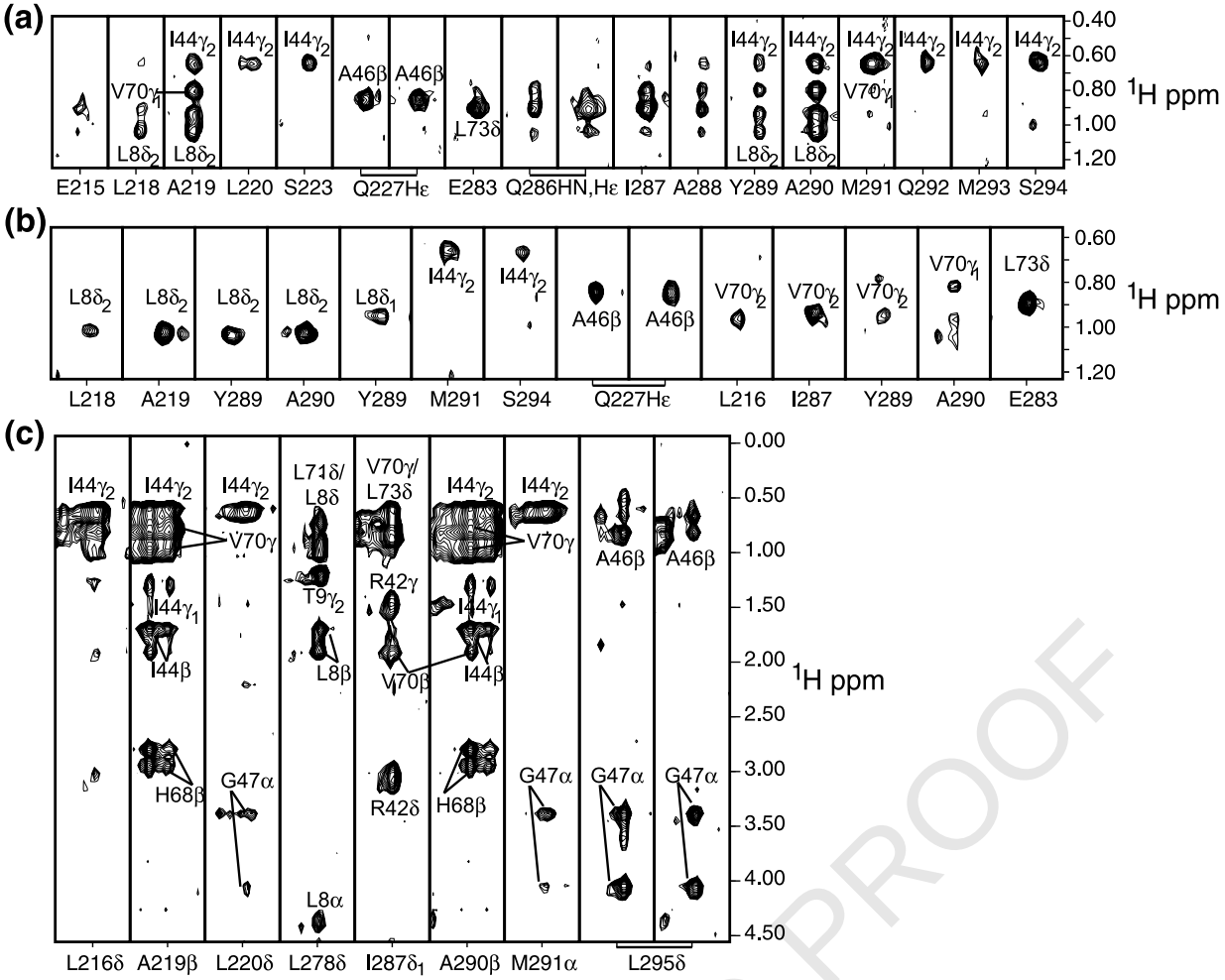

Figure 2. NOESY experiments reveal abundant contacts between S5a (196-306) and ubiquitin. (a) Selected ^{15}N planes from a 3D ^{15}N-dispersed NOESY recorded on $^{2}H,^{15}N$-labeled S5a (196-306) with unlabeled ubiquitin. (b) Selected ^{13}C planes from a 4D ^{15}N-edited ^{13}C-dispersed NOESY on $^{2}H,^{15}N$-labeled S5a (196-306) and ^{13}C-labeled ubiquitin. The dispersion in the ^{13}C dimension enabled the assignment of ubiquitin atoms at the S5a (196-306) contact surface. (c) Selected strips from a 3D ^{13}C-filtered ^{13}C-edited NOESY spectrum on a complex formed by ^{13}C-labeled S5a (196-306) and unlabeled ubiquitin. Labels inside and outside of the strips correspond to ubiquitin and S5a (196-306), respectively. In all cases the concentration of S5a (196-306) is 0.5 mM and its molar ratio with ubiquitin is 1:4.

experiment with a 200 ms mixing time, as this approach has been used with much success in studying other protein complexes.[20,31] Although this experiment was quite sensitive, and we were able to acquire over 50 NOE interactions, assigning the ubiquitin signals was not possible due to the limited dispersion of the ubiquitin side-chain proton resonances (Figure 2(a)). We therefore acquired a ^{13}C-dispersed, ^{15}N-edited NOESY on the sample containing ^{13}C-labeled ubiquitin. With the aid of the ^{13}C chemical-shift assignments we were able to assign all of the intermolecular NOE crosspeaks between ubiquitin side-chain protons and S5a (196-306) amide protons (Figure 2(b)). These assignments enabled us to assign the ^{15}N-dispersed NOESY on the complex with unlabeled ubiquitin (Figure 2(a)) and a ^{13}C half-filtered NOESY spectrum, which provided interactions between side-chain protons (Figure 2(c)).

In total, the three intermolecular NOESY experiments provided 115 distance constraints between S5a (196-306) and monoubiquitin (Figure 2). NOE interactions were observed between each of the UIMs of S5a and monoubiquitin, thereby establishing that each UIM can bind monoubiquitin. Indeed, only residues within the UIMs of S5a (196-306) contact ubiquitin, as no NOE interaction was observed with other parts of the protein. In addition, we found that neither ubiquitin nor S5a (196-306) experience gross structural changes upon binding. Our rationale for this assessment is twofold: namely, chemical-shift perturbation analysis on the free and complexed proteins identifies significant changes only for those residues at or near the interaction surfaces, and intramolecular NOE interactions for both ubiquitin and S5a (196-306) were unperturbed by forming the complex. On the basis of this conclusion, we solved the structure of the UIM/ubiquitin complexes by using experimental

Table 1. Structural statistics for the NMR structure of S5a (196-306) and its complex with ubiquitin

	S5a (196-306)	UIM-1/ubiquitin	UIM-2/ubiquitin
NOE distance restraints (total)	1371		
Inter-residue	834		
Medium-range	370		
$i,i+2$	100		
$i,i+3$	204		
$i,i+4$	66		
Long-range ($\|i-j\|>4$)	33		
Intermolecular		39	76
Hydrogen bonds	102		
Dihedral angle restraints (deg.)	120		
ϕ ($C'_{(i-1)} - N_i - C^{\alpha}_i - C'_i$)	70		
ϕ ($N_i - C^{\alpha}_i - C'_i - N_{(i+1)}$)	50		
Ramachandran plot			
Most-favorable region (%)	71.4	78.7	78.7
Additionally allowed region (%)	25.7	21.3	21.3
Generously allowed region (%)	2.6	0	0
Disallowed region (%)	0.3	0	0
r.m.s.d. for distance restraints (Å)	0.011 ± 0.002	0.009 ± 0.001	0.010 ± 0.001
r.m.s.d. for dihedral restraints (deg.)	0.114 ± 0.124	0.416 ± 0.021	0.425 ± 0.020
r.m.s.d. from ideal covalent geometry			
Bond lengths (Å)	$1.52(\pm 0.06)\times 10^{-3}$	$1.56(\pm 0.06)\times 10^{-3}$	$1.61(\pm 0.08)\times 10^{-3}$
Bond angles (deg.)	0.487 ± 0.006	0.498 ± 0.004	0.504 ± 0.005
Improper angles (deg.)	0.369 ± 0.010	0.385 ± 0.005	0.392 ± 0.006
r.m.s.d. of backbone atoms from av structure within regions of secondary structure (Å)	0.786 (P214-E245)	0.254[a]	0.219[b]
	0.142 (D257-E269)		
	0.348 (E283-Q296)		
r.m.s.d. of all heavy atoms from av structure within regions of secondary structure (Å)	1.352 (P214-E245)	0.695[c]	0.653[a]
	0.900 (D257-E269)		
	1.076 (E283-Q296)		

In the calculations of the complexes, intramolecular NOE distance and dihedral angle constraints are derived from the free proteins. The constraints for ubiquitin are obtained from Protein Data Bank 1D3Z.[48]

[a] Superimposing S5a E215-S223 and ubiquitin M1-V70.

[b] Superimposing S5a Q286-S294 and ubiquitin M1-V70.

[c] In the calculations of the complexes, intramolecular NOE distance and dihedral angle constraints are derived from the free proteins. The constraints for ubiquitin are obtained from Protein Data Bank 1D3Z.[48]

intramolecular constraints derived for the free proteins as well as the intermolecular NOE-derived distance constraints.

Structures of S5a UIM/ubiquitin complexes reveal basic requirements for binding ubiquitin

By using the data summarized in Table 1, we produced highly refined structures of ubiquitin complexed with UIM-1 or UIM-2 with root-mean-square deviations (r.m.s.d.) from averaged structures of <0.3 Å for the main-chain atoms (Figure 3). At the center of each ubiquitin-binding surface of S5a is the hydrophobic LALAL/IAYAM sequence, which characterizes UIMs. The residues in the first (L216/I287) and fourth positions (A219/A290) are highly conserved,[32] and it is these that form the strongest and most extensive NOE interactions with ubiquitin (Figure 2). Furthermore, these positions appear to be of general importance for binding UBL domains, as similar interactions exist between UIM-2 and analogous residues in the UBL domains of hHR23a and hHR23b.[22,23]

An additional residue that plays a prominent role in UIM binding to ubiquitin is a serine residue that forms a hydrogen bond with the backbone of G47 in ubiquitin: S223 in UIM-1 and S294 in UIM-2. The importance of this interaction is supported by the invariance of serine at this position among UIMs.[32] In addition, this hydrogen bond is likely conserved in UIM/UBL interactions, as this glycine position is conserved among UBL domains[17] and substitution of S294 with alanine leads to a 63-fold decrease in the binding affinity UIM-2 for hHR23b UBL.[23] In each of the UIM/ubiquitin complexes, the side-chain atoms of the long hydrophobic residue at position 5 of the LALAL/IAYAM repeat also contact G47 (Figure 2). These residues additionally form close contacts with I44 and are largely conserved among UIMs.[32]

Our structural data implicates the L···Aϕ···S sequence as required for ubiquitin binding, where ϕ symbolizes a bulky hydrophobic residue. Indeed, interactions between these residues and those of ubiquitin strictly define where the UIM α-helical regions contact ubiquitin, which results in an r.m.s.d. between UIM-1/ubiquitin and UIM-2/ubiquitin of 0.33 Å for the backbone atoms of ubiquitin and the α-helical region of each UIM.

Sequence comparisons implicate ede···L···A···S···e to be the overall UIM consensus.[32] The three moderately conserved N-terminal, negatively

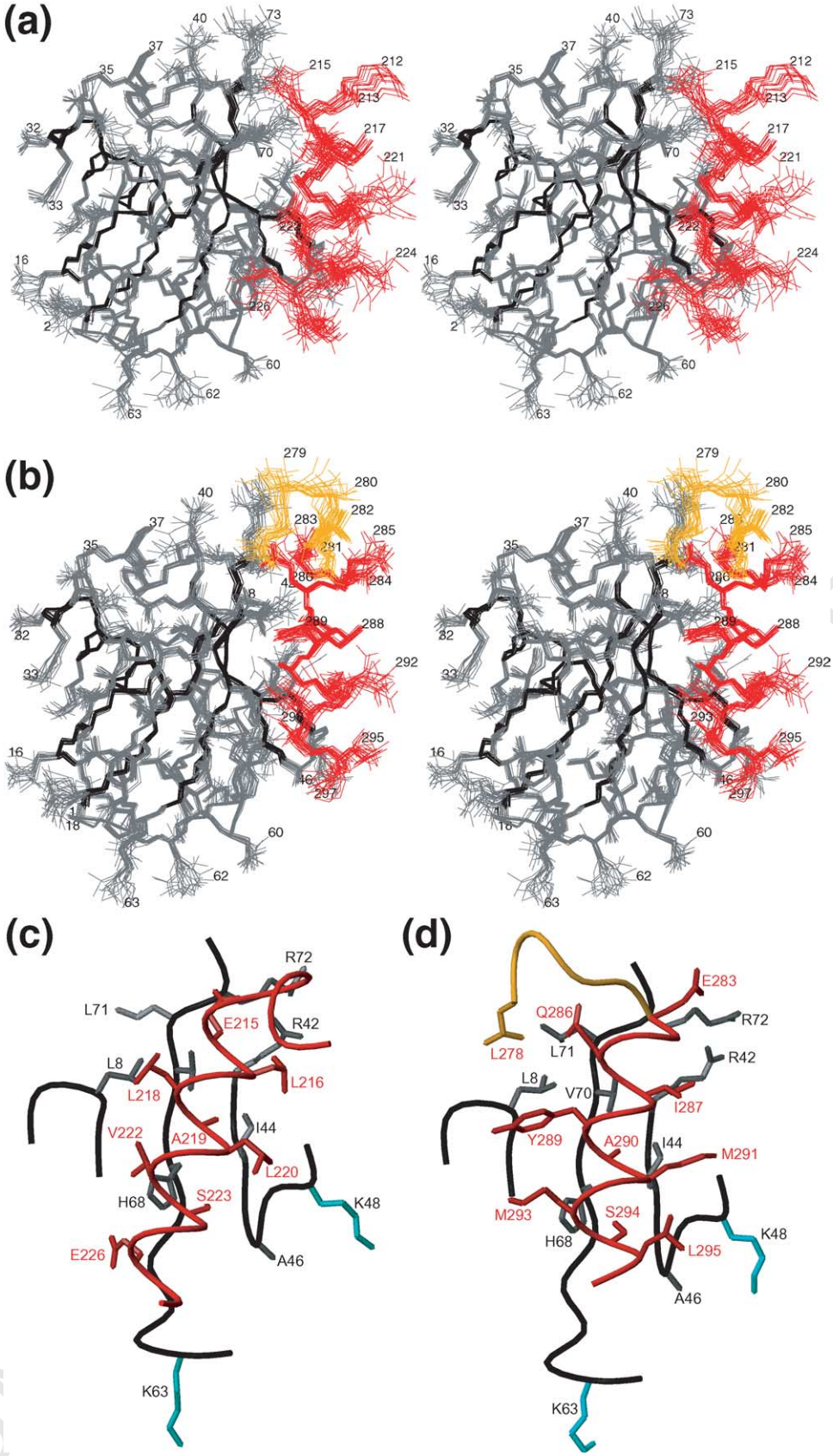

Figure 3. UIM-2 forms a more compact complex with monoubiquitin than does UIM-1. Stereo views are provided for the structures of ubiquitin (residues M1-L73) with (a) residues A212-Q227 of UIM-1 or (b) residues L278-Q296 of UIM-2 (b). Parts (c) and (d) highlight the interaction surfaces by providing a detailed view of the complexes shown in (a) and (b), respectively, and are rotated by ~45° relative to those in (a) and (b). In all parts of the Figure, the residues of UIM-1 (A212-Q227) and UIM-2 (E283-Q296) are colored red, and those in the turn of UIM-2 (L278-T282) are highlighted in orange. The backbone atoms of the secondary structural elements in ubiquitin are shown in black, and all other atoms are gray. This Figure was generated by using MOLMOL.[49]

charged residues in UIMs were demonstrated to contribute to ubiquitin binding.[29] However, we found that this region in UIM-1 does not interact directly with ubiquitin residues, and only two residues out of the three in UIM-2 (E283 and E284) form favorable electrostatic contacts with ubiquitin residues (R42 and R72). In the case of UIM-2, acidic residues in these two positions likely improve its binding affinity for ubiquitin by such direct contacts. However, the more general role of acidic residues N-terminal to the LALAL/IAYAM sequence may be to stabilize helix formation by forming favorable interactions with the helix dipole. In addition, the C-terminal acidic position is not conserved in UIM-2 and is therefore not required for ubiquitin binding. However, in UIM-1 it may improve its binding affinity for ubiquitin, as the side-chains of E226 and H68 of ubiquitin form a hydrogen bond, which is present also in the Vps27 UIM-1/ubiquitin complex.[30]

Compared with UIM-1, UIM-2 has a fivefold higher affinity for monoubiquitin

Although each of the UIMs of S5a bind ubiquitin, our structures show UIM-2 to form a more compact and extensive binding interface with ubiquitin. This finding is supported by UIM-2 being estimated to have at least tenfold higher affinity for polyubiquitin compared with UIM-1.[25] To test quantitatively our hypothesis that UIM-2 is the preferred ubiquitin-binding partner, we recorded ^{1}H,^{15}N heteronuclear single quantum coherence (HSQC) spectra on ^{15}N-labeled S5a (196-306) with increasing quantities of unlabeled ubiquitin. The analysis of the chemical-shift perturbations of selected residues within each UIM demonstrates that UIM-2 has a higher affinity for monoubiquitin than does UIM-1 (see Figure S2 in Supplementary Data). With the K_d value of 73 μM for UIM-2/monoubiquitin binding,[33] we find the K_d for UIM-1/monoubiquitin binding to be ~350 μM. Thus, this finding indicates that increased affinity of UIM-2 over UIM-1 for polyubiquitin is reflected in, and perhaps defined by, their intrinsic affinities for monoubiquitin.

Key structural differences account for the more compact ubiquitin binding of UIM-2

The increased binding affinity of UIM-2 over UIM-1 for ubiquitin can be attributed to several key structural differences. Firstly, in UIM-2/ubiquitin, Y289 forms favorable van der Waals interactions with L8 of ubiquitin (Figure 3(d)). The general importance of this tyrosine residue is suggested by the similar role it performs when UIM-2 is complexed with the UBL domain of hHR23b. This UBL domain has an analogous leucine residue that forms close contacts with Y289, which culminates in a hydrogen bond between its backbone carbonyl oxygen atom and the side-chain hydroxyl group of Y289.[23] In contrast, the analogous leucine of UIM-1 (L218) is unable to fulfil the role of Y289, due to its shorter side-chain (Figure 3(c)). Similarly, the analogous residue in UIM-1 of Vps27, K265 (Figure 1(a)), lacks NOE interactions with ubiquitin,[30] as its placement proximal to L8 would result in unfavorable electrostatic interactions.

The unique N-terminal region of UIM-2 is perhaps more important for binding ubiquitin than the favorable positioning of Y289. This region, which includes P276-T282, caps the ubiquitin hydrophobic surface formed by L8, V70, and L71 (Figure 3(d)). M281 is one of the key residues involved in stabilizing the N-terminal turn of UIM-2 and its substitution by alanine reduces polyubiquitin binding dramatically.[34] Hence, polyubiquitin likely uses a binding mechanism similar to that reported here for monoubiquitin, and the disparate N-terminal regions of the two UIMs likely contributes to the stronger interaction of UIM-2 with monoubiquitin (see above) and polyubiquitin.[25]

Another factor that favors UIM-2 interaction is the relative positioning of the LALAL/IAYAM sequence. In contrast with UIM-1, there is one full helical turn N-terminal to this sequence in UIM-2 (Figures 1 and 3). From within this configuration, E283 forms close contacts with R42 and R72 of ubiquitin. In contrast, in UIM-1 of S5a the analogous residue is A212, and the nearby negatively charged residue D213 is much further away from ubiquitin due to the bending caused by P210 and P214. As discussed below, this feature may contribute to the UBL domain of hPLIC family member ubiquilin binding to UIM-1 rather than UIM-2.[24]

S5a can bind either K48-linked or K63-linked polyubiquitin and prefers longer chains

The structure of monoubiquitin complexed with each S5a UIM reveals that the lysine residues of ubiquitin reside outside of its UIM interaction surface and we therefore hypothesized that S5a can bind polyubiquitin chains of any lysine linkage. Indeed, S5a was reported to bind chains linked through K6 and K11 in addition to the well-studied K48-linked chains.[35] Furthermore, K63-linked chains can signal proteasome-mediated protein degradation,[12] and indeed can be bound by hHR23a, although with a lower affinity compared with K48-linked chains.[36] In support of our hypothesis, we calculated structural models of S5a (196-306) bound to K29-linked, K48-linked and K63-linked tetraubiquitin, and found that none of our experimentally derived NOE constraints is violated in these complexes.

Furthermore, we tested our hypothesis experimentally by assessing whether affinity-purified His-tagged S5a (196-306) interacts with K48-linked or K63-linked polyubiquitin (Figure 4). Indeed, these experiments reveal that S5a (196-306) can bind either K48-linked or K63-linked polyubiquitin. More importantly, longer polyubiquitin chains are strongly preferred by S5a (196-306), as no detectable amount of monoubiquitin and comparatively little

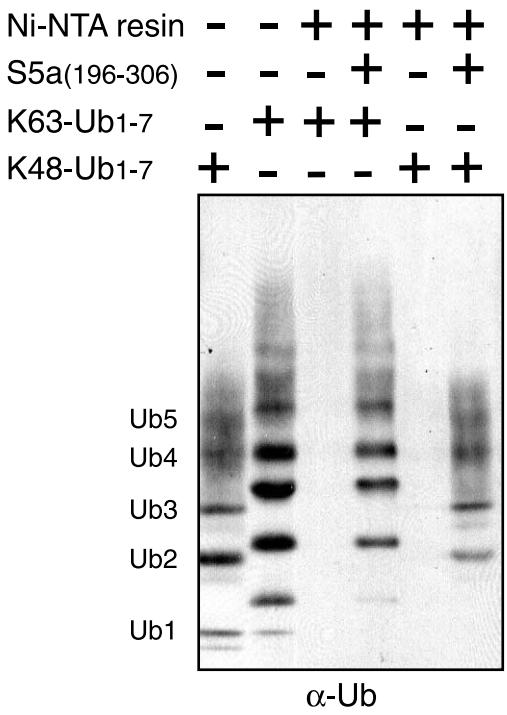

Figure 4. S5a (196-306) binds both K48-linked and K63-linked polyubiquitin chains. His-S5a (196-306) on Ni-NTA resin was incubated for two hours with 5 μg of either K48-linked or K63-linked polyubiquitin with a chain length ranging from one to seven (BostonBiochem Inc.). Proteins were fractionated on gels, transferred to a membrane and then probed with α-ubiquitin. Samples of the input polyubiquitin chains used in these experiments are provided on the left.

diubiquitin is pulled down by S5a (196-306)-bound resin (Figure 4).

Discussion

Structural basis for specific interactions with ubiquitin/UBL domain proteins

We have solved the structure of S5a (196-306) to reveal that UIM-1 begins a long α-helix that does not interact with the rest of the protein. UIM-1 differs from UIM-2 in its N-terminal region, structural location of the LALAL/IAYAM sequence, and in specific amino acid residues within the ubiquitin contact surface (Figure 1). These changes result in a less compact UIM-1/ubiquitin complex and in UIM-2 being the preferred ubiquitin-binding partner. In particular, our analysis reveals UIM-2 to have a fivefold increase in its binding affinity for monoubiquitin compared with UIM-1 (see Figure S2 in Supplementary Data).

The differences that result in UIM-2 rather than UIM-1 being the preferred ubiquitin-binding partner impact the UBL domain-binding capabilities of S5a even more dramatically. In particular, the UBL domain of the hPLIC family member ubiquilin binds only UIM-1,[24] whereas that of hHR23a binds only UIM-2.[19] By using our UIM/ubiquitin models, we produced model structures of the hPLIC-2 UBL domain complexed with either UIM-1 or UIM-2. The published structure of the UBL domain of hPLIC-2 reveals its last β-strand to be shorter than that of ubiquitin.[37] In addition, this strand is followed immediately by a lysine residue (K103), which in our model structures is able to form favorable electrostatic interactions with D213 of UIM-1 but has unfavorable steric clashes with E283 and E284 of UIM-2. Such distinctions may play an important role in embryonic development, as a truncated S5a isoform that lacks UIM-2 (Rpn10e) is expressed ubiquitously only in embryos.[38]

Model for polyubiquitin-recognition

Between the UIMs of S5a is a second α-helix with flexible linker regions at either end (Figure 1). This finding is significant because both UIMs of S5a are involved in binding polyubiquitin, since wild-type S5a binds almost tenfold more polyubiquitin than do constructs in which one of its UIMs is inactivated.[25] We expect that the flexible linkers separating the UIMs allow S5a to be highly adaptive for binding polyubiquitin chains. To test this hypothesis, we used our NOE data for S5a (196-306) complexed with monoubiquitin to produce structural models of S5a-tetraubiquitin (Figure 5). In the first published crystal structure of K48-linked tetraubiquitin, the UIM-binding surface is exposed in only the two distal ubiquitin moieties: Ub3 and Ub4 (Figure 5(a)).[39] Indeed, S5a can bind this tetraubiquitin structure in accordance with our experimental NOE constraints without introducing any steric violation.

The UIMs of S5a can span distances of up to ~140 Å. This feature may play an important role in defining the preference of S5a for longer polyubiquitin chains. Indeed, it enables the two UIMs to take full advantage of the increased binding volume and number of binding sites in longer polyubiquitin chains. Such an advantage is not afforded to binding very short chains. For example, to bind both ubiquitin moieties of diubiquitin simultaneously, in which the distance between the two moieties is small, S5a must adopt a rigid conformation and bring its two UIMs relatively close to each other.

Interestingly, hHR23 proteins, which are also well-known ubiquitin receptor proteins, have striking similarities with S5a. Like S5a, hHR23a has long flexible linker regions separating its two ubiquitin-associated (UBA) domains.[20,21] Therefore, it too may benefit from the increased binding volume and number of binding sites available in longer polyubiquitin chains. Indeed, the preference of S5a[15] and hHR23a[36] for longer chains is well established, and binding studies suggest that the two ubiquitin-binding sites in these proteins bind polyubiquitin cooperatively.[25,36] Such cooperativity

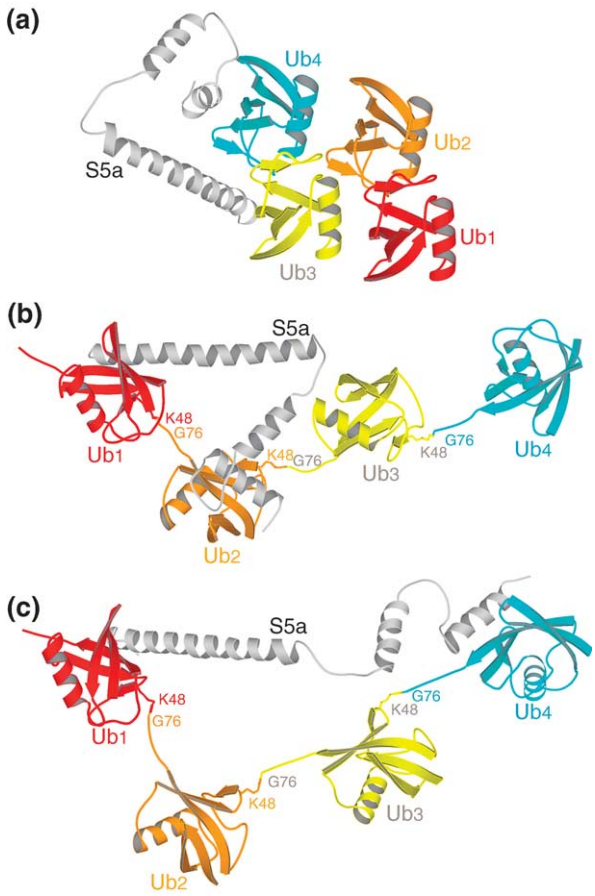

Figure 5. S5a flexible regions allow adaptable binding to tetraubiquitin. In (a) K48-linked tetraubiquitin from a crystal structure (PDB code 1TBE)[39] binds each of the UIMs of S5a *via* its two distal ubiquitin moieties. A snapshot of the two UIMs contacting either (b) neighboring or (c) terminal ubiquitin moieties is provided for K48-linked tetraubiquitin, in which the ubiquitin subunits are not forced to contact each other. The ubiquitin moieties are numbered sequentially according to the position of a hypothetical protein substrate: Ub1 (colored red) would be attached to a protein substrate *via* its G76. This Figure was generated by using MOLSCRIPT.[50]

could occur if binding to one ubiquitin moiety induces a conformational change in polyubiquitin that results in additional moieties being accessible for binding. In fact, the existence of such extended structures for tetraubiquitin is supported by the results of NMR experiments, which reveal its inter-subunit orientation to be dynamic,[40] and by crystal structures in which it adopts an extended conformation.[41]

We used structural modeling to assess whether the UIMs of S5a can bind any pair of subunits simultaneously in such an extended tetraubiquitin structure. In particular, we used our experimental data on S5a (196-306) binding to monoubiquitin to generate structures of its complex with K48-linked tetraubiquitin. In these structures, the ubiquitin moieties lack defined inter-subunit contacts. We found that the UIMs of S5a can bind neighboring or remote subunits without inducing any NOE violation (Figure 5(b) and (c)).

Model of how S5a and hHR23 recruit ubiquitylated substrates to the proteasome

The preference of hHR23a and S5a for longer polyubiquitin chains likely causes their signaling to be prioritized over shorter ones. In addition, hHR23a is able to establish a hierarchy in poly-ubiquitin chain signaling according to chain linkage. In particular, hHR23a confers specificity for K48-linked chains,[42] and structural analysis of its complex with ubiquitin provides an explanation for this observation. In contrast to the ubiquitin binding surface of S5a UIMs, which does not incorporate any lysine residue, that of hHR23a includes K48.[21] More importantly, hydrophobic residues of the UBA domains are proximal to the side-chain atoms of K48: L199 of UBA1 and L356 of UBA2.[43] This placement of hydrophobic side-chains proximal to a positive charge is unfavorable and the isopeptide bond in K48-linked chains results in the removal of this charge. We show here that the ubiquitin-binding surface of S5a is smaller and does not incorporate K48 (Figure 3). Indeed K63-linked chains serve as competent proteolytic signals,[12] and such signaling could occur *via* S5a (Figure 4).

Indeed, the ubiquitin receptor proteins S5a and hHR23a/b likely each contribute to determining the outcome of ubiquitylation. But could it be a coincidence that these and other ubiquitin receptor proteins interact? One tantalizing idea is that S5a collaborates with hHR23 to deliver ubiquitylated substrates to the proteasome. An S5a/hHR23 complex contains three possible ubiquitin-binding sites, as S5a binds hHR23a/b *via* its UIM-2, leaving UIM-1 and the two UBA domains available for binding ubiquitin moieties (Figure 6). This complex with its additional ubiquitin-binding sites and larger binding volume likely binds polyubiquitin with higher affinity and exhibits a stronger preference for longer chains than either protein alone. Perhaps S5a and hHR23 proteins, which serve as alternative ubiquitin receptors in yeast, increase their effectiveness and preference for polyubiquitin in humans by collaborating.

Materials and Methods

NMR spectroscopy

S5a (196-306), S5a (263-307), S5a (107-241), S5a (107-306) and ubiquitin were expressed and purified as described.[21,25] Chemical-shift assignments for S5a (196-306) were obtained by using modern NMR techniques.[26] Distance constraints for S5a (196-306) were obtained by using a 3D ^{15}N-dispersed NOESY spectrum (120 ms mixing time) as well as 3D ^{13}C-dispersed (80 ms mixing time) and 2D homonuclear NOESY (80 and 150 ms mixing times) spectra recorded in $^{2}H_2O$. Backbone ϕ and ϕ torsion angle constraints were derived by

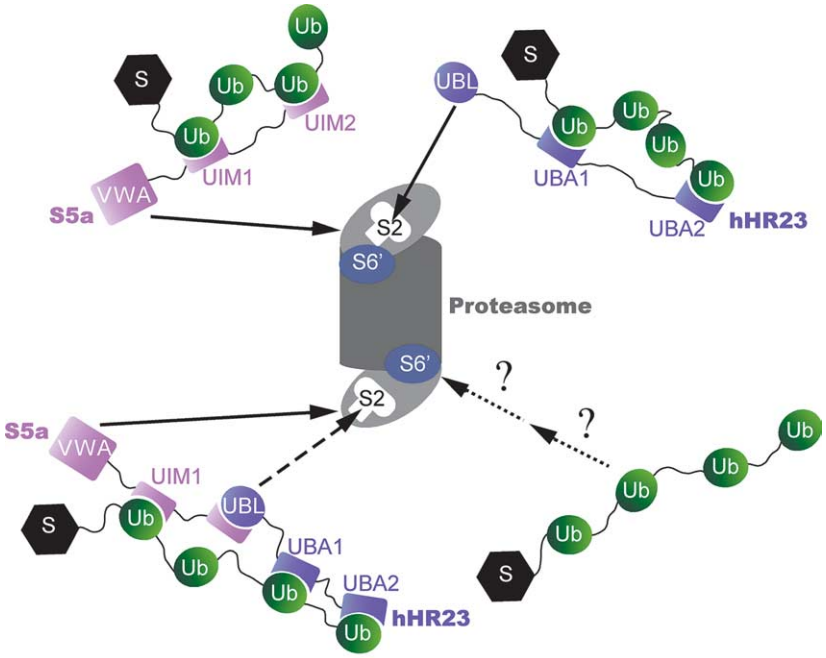

Figure 6. Potential mechanisms for delivering ubiquitylated substrates to the proteasome. S5a and hHR23 may function independently or collaboratively to deliver ubiquitylated substrates to the proteasome for their degradation. Each of these proteins contains two ubiquitin-binding elements that are connected by flexible linker regions.

using an HNHA spectrum,[44] and the program TALOS.[45] All spectra were acquired at 25 °C on either Varian 800 MHz or 600 MHz NMR spectrometers. Spectra were processed by NMRPipe,[46] and visualized in XEASY.[47]

To compare the relative binding affinities of the two S5a UIMs, we acquired ^{1}H,^{15}N HSQC spectra on ^{15}N-labeled S5a (196-306) at molar ratios of 2:1, 1:1, 1:2, and 1:4 with unlabeled ubiquitin. Chemical-shift perturbations (*CSP*) relative to free S5a (196-306) were calculated for selected residues (V208, D209, S211, A212, E215, L218, and S223 in UIM-1; L278 to Q286, A288, and S294 in UIM-2) according to equation (1) for each molar ratio:

$$CSP = \sqrt{0.2\Delta\delta_N^2 + \Delta\delta_H^2} \quad (1)$$

In this equation, $\Delta\delta_N$ and $\Delta\delta_H$ represent the changes in the amide nitrogen and proton chemical shifts (in parts per million), respectively. These values were normalized by the chemical shift perturbations of S5a (196-306) when in the presence of fourfold molar excess ubiquitin (equation (2)) and then plotted (see Figure S2 in Supplementary Data):

$$||CSP|| = \frac{CSP}{CSP_{4x\ \text{molar excess ubiquitin}}} \quad (2)$$

We simulated ||*CSP*|| by assuming *CSP* is proportional to the bound fraction of UIM as summarized in equation (3) and by using equation (4):

$$||CSP||_{UIM} = \frac{\left(\frac{[UIM_{bound}]}{[UIM_{total}]}\right)}{\left(\frac{[UIM_{bound}]}{[UIM_{total}]}\right)_{4x\ \text{molar excess ubiquitin}}} \quad (3)$$

$$[Ub_{total}] = [Ub_{free}] + [UIM1_{bound}] + [UIM2_{bound}] \quad (4)$$

Equation (4) can be rewritten as equation (5), in which K_d^{UIM-2} is the dissociation constant for UIM-2/ubiquitin binding and α is the ratio of the UIM-1/ubiquitin dissociation constant over that of UIM-2:

$$[Ub_{total}] = [Ub_{free}] + \frac{[Ub_{free}] \times [S5a(196-306)_{total}]}{K_d^{UIM-2} + [Ub_{free}]} + \frac{[Ub_{free}] \times [S5a(196-306)_{total}]}{\alpha \times K_d^{UIM-2} + [Ub_{free}]} \quad (5)$$

We simulated ||*CSP*|| at values for α of 5, 10 and 20 to find a good fit to our experimental data at $\alpha = 5$.

Intermolecular NOE interactions between S5a (196-306) and ubiquitin were obtained through three sets of NOESY experiments. In one case, an ^{15}N-dispersed NOESY spectrum (200 ms mixing time) was recorded on a sample containing ^{2}H,^{15}N-labeled S5a (196-306) with unlabeled ubiquitin. In the resulting spectrum, all amide to aliphatic NOE cross-peaks are exclusively intermolecular.[31] In addition, a ^{13}C-dispersed, ^{15}N-edited NOESY (200 ms mixing time) was acquired on ^{2}H,^{15}N-labeled S5a (196-306) with ^{13}C-labeled ubiquitin. In such a spectrum, all NOEs are intermolecular and the additional dispersion afforded by the ^{13}C dimension enabled the assignment of ubiquitin side-chain atoms at the contact surface. Furthermore, a 3D ^{13}C-filtered, ^{13}C-edited NOESY spectrum (100 ms mixing time) was obtained on a complex formed by ^{13}C-labeled S5a (196-306) and unlabeled ubiquitin. In all three spectra, the concentration of S5a (196-306) was 0.5 mM and its molar ratio with ubiquitin was 1:4.

Structure calculations

Structure calculations on S5a (196-306) were performed based on the NOE-derived distance and dihedral angle constraints (Table 1). Simulated annealing in XPLOR version 3.851 was performed on R12000 Octane Silicon Graphics workstations. A total of 15 random structures were subjected to 100,000 simulated annealing and cooling steps of 0.005 ps. All of these structures converged with no NOE violation >0.3 Å and no dihedral angle violation $>5°$.

For the complexes of ubiquitin with S5a (196-306), we used our intramolecular constraints for S5a (196-306) and

those published for ubiquitin (PDB code 1D3Z)[48] to maintain the structure of each component, as neither protein undergoes gross structural change upon binding (see Results). These constraints were combined with intermolecular NOE-derived distance constraints to calculate each complexed structure separately. Twenty random structures were subjected to 140,000 simulated annealing and cooling steps of 0.005 ps to generate 18 converged structures with no NOE violation >0.5 Å or dihedral angle violation $>5°$.

For the S5a-tetraubiquitin structural models, we used either a fixed crystal structure for tetraubiquitin (PDB code 1TBE)[39] or created tetraubiquitin from four mono-ubiquitin molecules (coordinates from PDB code 1D3Z),[48] which were linked through K48, K63, or K29. In both cases, NOE-derived constraints based on either free S5a (196-306) or its complex with monoubiquitin defined the structural integrity of S5a (196-306) and the interaction surfaces, respectively. In the tetraubiquitin structures, although the moieties were not constrained relative to each other, their structural integrity was maintained by using published constraints for free ubiquitin (PDB code 1D3Z).[48] Of the 20 structures subjected to simulated annealing, none of them exhibited violations in their intermolecular NOE constraints >0.5 Å.

Ubiquitin binding assay

Purified His-tagged S5a (196-306) was bound to pre-washed Ni-NTA resin in buffer A (20 mM sodium phosphate (pH 6.5), 100 mM NaCl, 0.5% (v/v) Triton X-100) for a final concentration of 9 μM. A sample (50 μl) of a 50% (w/w) slurry containing resin with bound His-S5a (196-306) was then mixed with 5 μg of either K63-linked or K48- linked polyubiquitin of chain length ranging from one to seven (BostonBiochem Inc.), in a total volume of 500 μl, in buffer A plus 1 mg/ml of bovine serum albumin. After incubation for two hours at 4 °C, each resin was pelleted and washed extensively with 1 ml of buffer A or buffer B (20 mM Tris–HCl (pH 7.6), 300 mM NaCl, 0.5% Triton X-100). To test for non-specific interactions involving polyubiquitin and the resin, a control experiment was performed under identical conditions by mixing each polyubiquitin mixture with Ni-NTA resin lacking S5a (196-306). Samples were fractionated by electrophoresis in a polyacrylamide gel and transferred to an Immobilon P membrane, which was probed with a polyclonal α-ubiquitin antibody (Boston-Biochem Inc.), followed by α-rabbit-horseradish peroxidase, and developed by ECL.

Data Bank accession numbers

The atomic coordinates have been deposited in the Protein Data Bank for S5a (196-306) alone (PDB 1YX4) as well as in complex with ubiquitin (PDB 1YX5 for UIM-1 and 1YX6 for UIM-2).

Acknowledgements

We are grateful to Yang Kang for assisting with the sample preparation, to Dr Yuk Y. Sham for his assistance with the XPLOR calculations, and to Lin Ma, Dr Howard Towle, and Dr Hiroshi Matsuo for their help with the Western experiments. NMR data were acquired at the NMR facility of the University of Minnesota and we thank Dr David Live and Dr Beverly Ostrowsky for their technical assistance. NMR instrumentation was provided with funds from the NSF (BIR-961477), the University of Minnesota Medical School, and the Minnesota Medical Foundation. Data processing and visualization were performed in the Basic Sciences Computing Lab of the University of Minnesota Supercomputing Institute. This work was funded by a grant from the National Institutes of Health CA097004-01A1 (to K.J.W.).

Supplementary Data

Supplementary data associated with this article can be found, in the online version, at doi:10.1016/j.jmb.2005.03.007

References

1. Ciechanover, A. (1994). The ubiquitin-proteasome proteolytic pathway. *Cell*, **79**, 13–21.
2. Hicke, L. (2001). A new ticket for entry into budding vesicles-ubiquitin. *Cell*, **106**, 527–530.
3. Katzmann, D. J., Odorizzi, G. & Emr, S. D. (2002). Receptor downregulation and multivesicular-body sorting. *Nature Rev. Mol. Cell Biol.* **3**, 893–905.
4. Conaway, R. C., Brower, C. S. & Conaway, J. W. (2002). Emerging roles of ubiquitin in transcription regulation. *Science*, **296**, 1254–1258.
5. Muratani, M. & Tansey, W. P. (2003). How the ubiquitin-proteasome system controls transcription. *Nature Rev. Mol. Cell Biol.* **4**, 192–201.
6. Hoege, C., Pfander, B., Moldovan, G. L., Pyrowolakis, G. & Jentsch, S. (2002). RAD6-dependent DNA repair is linked to modification of PCNA by ubiquitin and SUMO. *Nature*, **419**, 135–141.
7. Spence, J., Sadis, S., Haas, A. L. & Finley, D. (1995). A ubiquitin mutant with specific defects in DNA repair and multiubiquitination. *Mol. Cell. Biol.* **15**, 1265–1273.
8. Yamaguchi, R. & Dutta, A. (2000). Proteasome inhibitors alter the orderly progression of DNA synthesis during S-phase in HeLa cells and lead to rereplication of DNA. *Expt. Cell Res.* **261**, 271–283.
9. Wolf, D. H., Sommer, T. & Hilt, W. (2004). Death gives birth to life: the essential role of the ubiquitin-proteasome system in biology. *Biochim. Biophys. Acta*, **1695**, 1–2.
10. Pickart, C. M. (2000). Ubiquitin in chains. *Trends Biochem. Sci.* **25**, 544–548.
11. Hofmann, R. M. & Pickart, C. M. (1999). Noncanonical MMS2-encoded ubiquitin-conjugating enzyme functions in assembly of novel polyubiquitin chains for DNA repair. *Cell*, **96**, 645–653.
12. Hofmann, R. M. & Pickart, C. M. (2001). *In vitro* assembly and recognition of Lys-63 polyubiquitin chains. *J. Biol. Chem.* **276**, 27936–27943.
13. Elsasser, S., Chandler-Militello, D., Muller, B., Hanna, J. & Finley, D. (2004). Rad23 and Rpn10 serve as alternative ubiquitin receptors for the proteasome. *J. Biol. Chem.* **279**, 26817–26822.
14. Verma, R., Oania, R., Graumann, J. & Deshaies, R. J.

(2004). Multiubiquitin chain receptors define a layer of substrate selectivity in the ubiquitin-proteasome system. *Cell*, **118**, 99–110.
15. Deveraux, Q., Ustrell, V., Pickart, C. & Rechsteiner, M. (1994). A 26 S protease subunit that binds ubiquitin conjugates. *J. Biol. Chem.* **269**, 7059–7061.
16. van Nocker, S., Sadis, S., Rubin, D. M., Glickman, M., Fu, H., Coux, O. *et al*. (1996). The multiubiquitin-chain-binding protein Mcb1 is a component of the 26S proteasome in Saccharomyces cerevisiae and plays a nonessential, substrate-specific role in protein turnover. *Mol. Cell. Biol.* **16**, 6020–6028.
17. Walters, K. J., Goh, A. M., Wang, Q., Wagner, G. & Howley, P. M. (2004). Ubiquitin family proteins and their relationship to the proteasome: a structural perspective. *Biochim. Biophys. Acta*, **1695**, 73–87.
18. Lam, Y. A., Lawson, T. G., Velayutham, M., Zweier, J. L. & Pickart, C. M. (2002). A proteasomal ATPase subunit recognizes the polyubiquitin degradation signal. *Nature*, **416**, 763–767.
19. Hiyama, H., Yokoi, M., Masutani, C., Sugasawa, K., Maekawa, T., Tanaka, K. *et al*. (1999). Interaction of hHR23 with S5a. The ubiquitin-like domain of hHR23 mediates interaction with S5a subunit of 26 S proteasome. *J. Biol. Chem.* **274**, 28019–28025.
20. Walters, K. J., Lech, P. J., Goh, A. M., Wang, Q. & Howley, P. M. (2003). DNA-repair protein hHR23a alters its protein structure upon binding proteasomal subunit S5a. *Proc. Natl Acad. Sci. USA*, **100**, 12694–12699.
21. Wang, Q., Goh, A. M., Howley, P. M. & Walters, K. J. (2003). Ubiquitin recognition by the DNA repair protein hHR23a. *Biochemistry*, **42**, 13529–13535.
22. Mueller, T. D. & Feigon, J. (2003). Structural determinants for the binding of ubiquitin-like domains to the proteasome. *EMBO J.* **22**, 4634–4645.
23. Fujiwara, K., Tenno, T., Sugasawa, K., Jee, J. G., Ohki, I., Kojima, C. *et al*. (2004). Structure of the ubiquitin-interacting motif of S5a bound to the ubiquitin-like domain of HR23B. *J. Biol. Chem.* **279**, 4760–4767.
24. Seok Ko, H., Uehara, T., Tsuruma, K. & Nomura, Y. (2004). Ubiquilin interacts with ubiquitylated proteins and proteasome through its ubiquitin-associated and ubiquitin-like domains. *FEBS Letters*, **566**, 110–114.
25. Young, P., Deveraux, Q., Beal, R. E., Pickart, C. M. & Rechsteiner, M. (1998). Characterization of two polyubiquitin binding sites in the 26 S protease subunit 5a. *J. Biol. Chem.* **273**, 5461–5467.
26. Wang, Q. & Walters, K. J. (2004). Chemical shift assignments of the (poly)ubiquitin-binding region of the proteasome subunit S5a. *J. Biomol. NMR*, **30**, 231–232.
27. Realini, C., Rogers, S. W. & Rechsteiner, M. (1994). KEKE motifs. Proposed roles in protein-protein association and presentation of peptides by MHC class I receptors. *FEBS Letters*, **348**, 109–113.
28. Branden, C. & Tooze, J. (1999). *Introduction to Protein Structure* (2nd edit.), Garland Publishers, New York.
29. Fisher, R. D., Wang, B., Alam, S. L., Higginson, D. S., Robinson, H., Sundquist, W. I. & Hill, C. P. (2003). Structure and ubiquitin binding of the ubiquitin interacting motif. *J. Biol. Chem.* **278**, 28976–28984.
30. Swanson, K. A., Kang, R. S., Stamenova, S. D., Hicke, L. & Radhakrishnan, I. (2003). Solution structure of Vps27 UIM-ubiquitin complex important for endosomal sorting and receptor downregulation. *EMBO J.* **22**, 4597–4606.
31. Walters, K. J., Matsuo, H. & Wagner, G. (1997). A simple method to distinguish intermonomer NOEs in homodimeric proteins with C_2 symmetry. *J. Am. Chem. Soc.* **119**, 5958–5959.
32. Hofmann, K. & Falquet, L. (2001). A ubiquitin-interacting motif conserved in components of the proteasomal and lysosomal protein degradation systems. *Trends Biochem. Sci.* **26**, 347–350.
33. Ryu, K. S., Lee, K. J., Bae, S. H., Kim, B. K., Kim, K. A. & Choi, B. S. (2003). Binding surface mapping of intra- and interdomain interactions among hHR23B, ubiquitin, and polyubiquitin binding site 2 of S5a. *J. Biol. Chem.* **278**, 36621–36627.
34. Beal, R. E., Toscano-Cantaffa, D., Young, P., Rechsteiner, M. & Pickart, C. M. (1998). The hydrophobic effect contributes to polyubiquitin chain recognition. *Biochemistry*, **37**, 2925–2934.
35. Baboshina, O. V. & Haas, A. L. (1996). Novel multiubiquitin chain linkages catalyzed by the conjugating enzymes E2EPF and RAD6 are recognized by 26 S proteasome subunit 5. *J. Biol. Chem.* **271**, 2823–2831.
36. Raasi, S., Orlov, I., Fleming, K. G. & Pickart, C. M. (2004). Binding of polyubiquitin chains to ubiquitin-associated (UBA) domains of HHR23A. *J. Mol. Biol.* **341**, 1367–1379.
37. Walters, K. J., Kleijnen, M. F., Goh, A. M., Wagner, G. & Howley, P. M. (2002). Structural studies of the interaction between ubiquitin family proteins and proteasome subunit S5a. *Biochemistry*, **41**, 1767–1777.
38. Kawahara, H., Kasahara, M., Nishiyama, A., Ohsumi, K., Goto, T., Kishimoto, T. *et al*. (2000). Developmentally regulated, alternative splicing of the Rpn10 gene generates multiple forms of 26S proteasomes. *EMBO J.* **19**, 4144–4153.
39. Cook, W. J., Jeffrey, L. C., Kasperek, E. & Pickart, C. M. (1994). Structure of tetraubiquitin shows how multiubiquitin chains can be formed. *J. Mol. Biol.* **236**, 601–609.
40. Varadan, R., Walker, O., Pickart, C. & Fushman, D. (2002). Structural properties of polyubiquitin chains in solution. *J. Mol. Biol.* **324**, 637–647.
41. Phillips, C. L., Thrower, J., Pickart, C. M. & Hill, C. P. (2001). Structure of a new crystal form of tetraubiquitin. *Acta Crystallog. sect. D*, **57**, 341–344.
42. Raasi, S. & Pickart, C. M. (2003). Rad23 UBA domains inhibit 26S proteasome-catalyzed proteolysis by sequestering lysine 48-linked polyubiquitin chains. *J. Biol. Chem.* **278**, 8951–8959.
43. Kang, R. S., Daniels, C. M., Francis, S. A., Shih, S. C., Salerno, W. J., Hicke, L. & Radhakrishnan, I. (2003). Solution structure of a CUE-ubiquitin complex reveals a conserved mode of ubiquitin binding. *Cell*, **113**, 621–630.
44. Vuister, G. W. & Bax, A. (1993). Quantitative J correlation: a new approach for measuring homonuclear three-bond $J(H^NH^\alpha)$ coupling constants in ^{15}N-enriched proteins. *J. Am. Chem. Soc.* **115**, 7772–7777.
45. Cornilescu, G., Delaglio, F. & Bax, A. (1999). Protein backbone angle restraints from searching a database for chemical shift and sequence homology. *J. Biomol. NMR*, **13**, 289–302.
46. Delaglio, F., Grzesiek, S., Vuister, G. W., Zhu, G., Pfeifer, J. & Bax, A. (1995). NMRPipe: a multidimensional spectral processing system based on UNIX pipes. *J. Biomol. NMR*, **6**, 277–293.
47. Bartels, C., Xia, T.-H., Billeter, M., Güntert, P. &

Wüthrich, K. (1995). The program XEASY for computer-supported NMR spectral analysis of biological macromolecules. *J. Biomol. NMR*, **6**, 1–10.
48. Cornilescu, G., Marquardt, J. L., Ottiger, M. & Bax, A. (1998). Validation of protein structure from anisotropic carbonyl chemical shifts in a dilute liquid crystalline phase. *J. Am. Chem. Soc.* **120**, 6836–6837.
49. Koradi, R., Billeter, M. & Wüthrich, K. (1996). MOLMOL: a program for display and analysis of macromolecular structures. *J. Mol. Graph.* **14**, 51–55.
50. Kraulis, P. J. (1991). MOLSCRIPT: a program to produce both detailed and schematic plots of protein structures. *J. Appl. Crystallog.* **24**, 946–950.

Edited by M. F. Summers

(Received 27 January 2005; received in revised form 22 February 2005; accepted 1 March 2005)